

## Desformylgramicidin: A Model Channel with an Extremely High Water Permeability

Sapar M. Saparov,\* Yuri N. Antonenko,<sup>†</sup> Roger E. Koeppe II,<sup>‡</sup> and Peter Pohl\*

\*Martin-Luther-Universität, Medizinische Fakultät, Institut für Medizinische Physik und Biophysik, 06097 Halle, Germany, <sup>†</sup>A.N.Belozersky Institute of Physico-Chemical Biology, Moscow State University, Moscow 119899, Russia, <sup>‡</sup>Department of Chemistry and Biochemistry, University of Arkansas, Fayetteville, AR 72701, USA

**ABSTRACT** The water conductivity of desformylgramicidin exceeds the permeability of gramicidin A by two orders of magnitude. With respect to its single channel hydraulic permeability coefficient of  $1.1 \cdot 10^{-12} \text{ cm}^3 \text{ s}^{-1}$ , desformylgramicidin may serve as a model for extremely permeable aquaporin water channel proteins (AQP4 and AQPZ). This osmotic permeability exceeds the conductivity that is predicted by the theory of single-file transport. It was derived from the concentration distributions of both pore-impermeable and -permeable cations that were simultaneously measured by double barreled microelectrodes in the immediate vicinity of a planar bilayer. From solvent drag experiments, approximately five water molecules were found to be transported by a single-file process along with one ion through the channel. The single channel proton, potassium, and sodium conductivities were determined to be equal to 17 pS (pH 2.5), 7 and 3 pS, respectively. Under any conditions, the desformyl-channel remains at least 10 times longer in its open state than gramicidin A.

### INTRODUCTION

Peptides may be synthesized with sequences corresponding to putative transmembrane domains of ion channel proteins to serve after incorporation into lipid bilayers as models for structural and functional studies (Marsh, 1996). Gramicidin is used as a model for ion transport in biological membranes because the structures formed by gramicidin are among the best characterized of all membrane-bound polypeptides or proteins (Ketchum et al., 1997). Using the gramicidin channel as a model, it was, for example, tested whether a single strand of water is kinetically competent to translocate protons at a rate sufficient to support known rates of  $F_1-F_0$ -ATP synthesis (Akeson and Deamer, 1991). Also, the importance of membrane elastic deformations associated with a protein conformational change can be evaluated using gramicidin (Andersen et al., 1999a). The correlation between membrane tension and both the rate at which the gramicidin channel opens and its lifetime supports a phenomenological model of membrane elasticity in which tension modulates the mismatch in thickness between the gramicidin dimer and the membrane (Goulian et al., 1998). By replacing tryptophan residues in gramicidin A with the more polar 5-F-tryptophan, the interfacial location of the amphipathic aromatic amino acid residues tryptophan and tyrosine is shown to be significant for membrane protein structure and function (Busath et al., 1998; Andersen et al., 1998). The family of gramicidin channels has developed into a powerful model system for understanding fundamen-

tal properties, interactions, and dynamics of proteins and lipids generally, and ion channels specifically, in biological membranes (Greathouse et al., 1999).

Investigations of volume flow across the gramicidin channel have appeared to be very important for the interpretation of results obtained with protein channels. The transport of ions and water throughout most of the gramicidin channel length occurs in a single-file fashion; that is, cations and water molecules cannot pass each other within the channel (for reviews see Finkelstein and Andersen, 1981; Hladky and Haydon, 1984). Direct evidence was obtained that the presence of a cation in the channel reduces the hydraulic water permeability (Dani and Levitt, 1981a). The number of water molecules coupled to the transport of one cation via gramicidin was found to be in reasonable agreement with the channel length predicted from the peptide structure (Levitt et al., 1978; Rosenberg and Finkelstein, 1978a; Tripathi and Hladky, 1998). Following the procedure developed with gramicidin, the dimensions of the narrowest part of other channels were estimated, e.g., of  $K^+$ -selective channels from fragmented sarcoplasmic reticulum (Miller, 1982), of cardiac sarcoplasmic reticulum  $Ca^{2+}$  release channels (Tu et al., 1994) or of cloned epithelial  $Na^+$  channels incorporated into planar lipid bilayers (Ismailov et al., 1997).

Assuming that the gramicidin channel walls are a representative of uncharged polar protein surfaces, the hydraulic single-channel permeability coefficient,  $p_f$ , can be predicted from the length of the channel,  $L$ , the number of water molecules in the channel,  $N$ , their diffusion coefficient,  $D_w$ , the molar volume of water,  $V_w$  and the Avogadro-number,  $N_A$  (Finkelstein, 1987):

$$p_f = \frac{V_w D_w N}{N_A L^2} \quad (1)$$

Received for publication 3 April 2000 and in final form 1 August 2000.

Address reprint requests to Peter Pohl, Martin-Luther-Universität, Medizinische Fakultät, Institut für Medizinische Physik und Biophysik, 06097 Halle, Germany. Tel.: +49-345-5571243; Fax: +49-345-5571632; E-mail peter.pohl@medizin.uni-halle.de.

© 2000 by the Biophysical Society

0006-3495/00/11/2526/09 \$2.00

If it is assumed that (see, for example, Mathai et al., 1996)

$$L = 2.72 \cdot 10^{-10} \text{ m} \cdot N, \quad (2)$$

$D_w = 2.4 \cdot 10^{-5} \text{ cm}^2\text{s}^{-1}$  and  $N = 5$  (Rosenberg and Finkelstein, 1978b; Pohl and Saparov, 2000), a  $p_f$  of  $2 \cdot 10^{-13} \text{ cm}^3\text{s}^{-1}$  is obtained for gramicidin. For gramicidin channels imbedded in phospholipid membranes, the experimentally determined value is one order of magnitude smaller (Rosenberg and Finkelstein, 1978b; Pohl and Saparov, 2000).

Discrepancies between the single-channel permeability coefficient predicted from the theory (Eq. 1) and the experimental value have also been observed for Aquaporin 4, a water-channel protein (Yang et al., 1997). Similar to gramicidin, the aquaporins represent narrow channels where transport occurs as a single-file process (Walz et al., 1994). Aquaporin channel proteins facilitate water movement across the plasma membrane (Preston et al., 1992) with an unparalleled selectivity for water over ions. Failure to permit entry of uncharged solutes such as urea may be determined by the pore size, however this does not explain the failure to transport protons and cations that may be due to electrical filtering (Zeidel et al., 1994).

To gain more insight into the molecular mechanism of single-file water transport, gramicidin derivatives designed to have a higher water selectivity than gramicidin A may be very useful. After introducing a positive charge into the gramicidin peptide by synthesizing a desformyl compound, we have investigated the accompanying changes in water, cation, and proton permeabilities. Earlier, this derivative was reported to have cation permeability that is four orders of magnitude smaller than that of gramicidin A (Goodall, 1971), whereas the proton conductivities of both peptides are similar (Bezrukov et al., 1984). Now we have measured the single-channel permeability for protons, potassium, and water. Although desformylgramicidin has a higher water selectivity than gramicidin A, it is still far below the extreme water selectivity reported for aquaporins. The most plausible explanation is that the positive charge of the N-terminus is located at the membrane surface rather than in the center of a channel formed by dimers. In contrast to the hypothetical double-stranded dimer structure of the desformyl channel, gramicidin A forms a head-to-head dimer of two single-stranded  $\beta$ -helices (for review see Andersen et al., 1999b) that is connected by six hydrogen bonds between the formyl N-terminals (Koeppel and Andersen, 1996).

## MATERIALS AND METHODS

### Membranes

Planar black lipid membranes (BLMs) were formed from a 20-mg/ml solution of diphytanoyl phosphatidylcholine (DPhPC, Avanti Polar Lipids, Alabaster, AL) in *n*-decane (Mueller et al., 1963). They were spread across a circular hole in a diaphragm separating two aqueous phases of a polytetrafluorethylene chamber. Two different apertures with diameters of 0.8

and 1.6 mm were used. Gramicidin A (Sigma, Dreisenhofen, Germany) or desformylgramicidin were added at both sides of the BLM from an ethanolic stock solution. Desformylgramicidin was synthesized by the procedure of Weiss and Koeppel (1985). We note, however, that, with desformylgramicidin, we have been unable to achieve the very high purity that is characteristic of the uncharged gramicidins following multiple reversed-phase chromatographic purification steps (Weiss and Koeppel, 1985; Koeppel et al., 1985; Andersen et al., 1998).

All experiments were carried out at room temperature (23–24°C). The aqueous solutions of choline chloride (Merck, Darmstadt, Germany) were buffered with 20 mM Tris (Fluka, Buchs, Switzerland).

### Water flux measurements

Osmotic gradients were imposed by urea (Laborchemie Apolda, Apolda, Germany). This osmolyte has negligible effect on bulk viscosity. A membrane doped with gramicidin is impermeable for urea (Finkelstein, 1987). Also in the experiments with desformylgramicidin, urea was assumed to be a nonpenetrating solute, which is completely reflected by the membrane. The transmembrane water flow leads to accumulation of solutes on one side of the membrane and depletion on the other (Fettiplace and Haydon, 1980). From the resulting concentration distribution of an impermeant ion,  $c_i(x)$ , the velocity of transmembrane water flow,  $v_t$ , can be calculated (Pohl et al., 1997),

$$c_i(x) = c_{i,s} \exp\left(\frac{-v_t x}{D_i} + \frac{ax^3}{3D_i}\right), \quad (3)$$

where  $c_{i,s}$  and  $D_i$  are the surface concentration and the diffusion coefficient of the impermeant solute, respectively. Eq. 1 may be applied only in a region close to the membrane, where the product of the stirring parameter,  $a$ , and the square of the distance,  $x$ , to the membrane is smaller than the velocity of transmembrane water flow,  $v_t$ .

The transmembrane flux of a permeant ion,  $J_m$ , can be found both from the transmembrane current and from its near-membrane concentration distribution,  $c_{p,s}$ , provided that  $v_t$  is known (Pohl and Saparov, 2000):

$$c_p(x) = \frac{J_m}{v_t} + \left(c_{p,s} - \frac{J_m}{v_t}\right) e^{-v_t x/D_p}. \quad (4)$$

Eq. 2 works in a region very close to the membrane, where the condition  $v_t \gg ax^2$  is fulfilled. It is assumed that the concentration of the permeable solute,  $c_p$ , reaches the value  $c_{p,s}$  at the membrane surface ( $x = 0$ ).

In the immediate vicinity of the membrane, the spatial distributions of both permeant and impermeant ions were monitored simultaneously. The experimental arrangement was similar to the one described previously (Antonenko et al., 1993; Pohl et al., 1993). In brief, a double-barreled microelectrode and a reference electrode were placed at the *trans* side of the BLM. The ion sensitivity was achieved by filling both glass barrels with ionophore cocktails (Sodium Ionophore II Cocktail A, Calcium Ionophore I Cocktail A, and Potassium Ionophore I Cocktail B, Fluka, Buchs, Switzerland) according to the procedure described by Amman (1986). Their tips had a diameter of  $\sim 1$ – $2 \mu\text{m}$ .

Voltage sampling of electrode potentials was performed by two electrometers (Model 617, Keithley Instruments Inc., Cleveland, OH) connected via an IEEE-interface to a personal computer. The double-barreled microelectrode was moved perpendicular to the surface of the BLM by a hydraulic microdrive manipulator (Narishige, Tokyo, Japan). The touching of the membrane was indicated by a steep potential change (Antonenko and Bulychev, 1991). From the known velocity of the electrode motion ( $2 \mu\text{m s}^{-1}$ ), the position of the microsensor relative to the membrane was determined at any instant of the experiment. Artifacts due to the slow electrode movement are unlikely because the response of the electrode potential to concentration changes occurred comparatively fast, i.e., the 90% rise time was below 0.6 s. Nevertheless, possible effects of time resolution or

distortion of the unstirred layer were tested by making measurements while moving the microelectrode toward and away from the bilayer. Since no hysteresis was found, it can be assumed that an electrode of appropriate time resolution was driven without any effect on the USL. The accuracy of the distance measurements was estimated to be  $\pm 8 \mu\text{m}$ . During the experiments, the buffer solutions were continuously agitated by magnetic stirrer bars.

## Measurements of transmembrane current and membrane conductance

To monitor the current under short-circuited conditions, Ag/AgCl-pellets that were connected to a picoamperemeter (Model 428, Keithley Instruments Inc., Cleveland, OH) were immersed into the bathing buffer solutions at both sides of the membrane. The amplified signal was visualized by a voltmeter.

Membrane conductance was monitored just before and just after the volume flux measurement. Two pairs of electrodes were exploited. The first pair of Ag/AgCl pellets was used to record a current step. A 1-kHz square wave input voltage (source: Model 33120A, Hewlett-Packard, Loveland, CO) was applied to the membrane. The output signal was first amplified by a picoamperemeter (Model 428, Keithley Instruments Inc.) and then transferred to an oscilloscope (model TDS 340, Tektronix Inc., Wilsonville, OR). Through the second pair of pellets, the resulting potential difference was recorded by an operational amplifier (AD549, Analog Devices, Norwood, MA) and displayed on the second channel of the oscilloscope.

## Single-channel conductance measurements

For single-channel current measurements, a small fragment of the membrane was electrically isolated from the rest of the bilayer as described earlier (Antonenko and Pohl, 1998). In brief, a glass pipette was placed on the *cis* bilayer surface where it formed a stable gigaohm seal. Before the experiments, the tips of the glass capillaries had been thinned by a puller (model PP-83, Narishige) to a diameter of about  $5 \mu\text{m}$ . To approach the bilayer, the pipettes were moved perpendicular to the surface of the BLM by a hydraulic microdrive manipulator (Narishige). The touching of the membrane was observed with the help of a microscope. Reference electrodes were inserted into the pipette and into the buffer solution at the *trans* side of the BLM. To monitor the current across the voltage-clamped membrane fragment inside the pipette, a patch-clamp amplifier was used (EPC-9, HEKA Electronics, Lambrecht, Germany). The sampling frequency was fixed at 0.5 kHz. The recording filter was a 4-pole Bessel with 3-dB corner frequency of 0.1 kHz. The acquired raw data were analyzed with the help of the TAC software package (Bruyton Corporation, Seattle, WA). To reduce noise, a Gaussian filter of 37 Hz was applied.

## RESULTS

### Water and ion fluxes across desformylgramicidin channels

Insertion of both gramicidin A and desformylgramicidin channels into the planar bilayer enhanced the initial osmotic water flux,  $J_{W,l}$ , as revealed by the large polarization of membrane-impermeable calcium ions observed in the immediate membrane vicinity (Fig. 1). The additional water flux that is introduced by the porous pathway,  $J_{W,c}$  was calculated from the  $\text{Ca}^{2+}$  concentration profiles. Therefore,  $v_t$  was obtained by fitting the parametric Eq. 1 to the experimental data set. For the minimization of the least

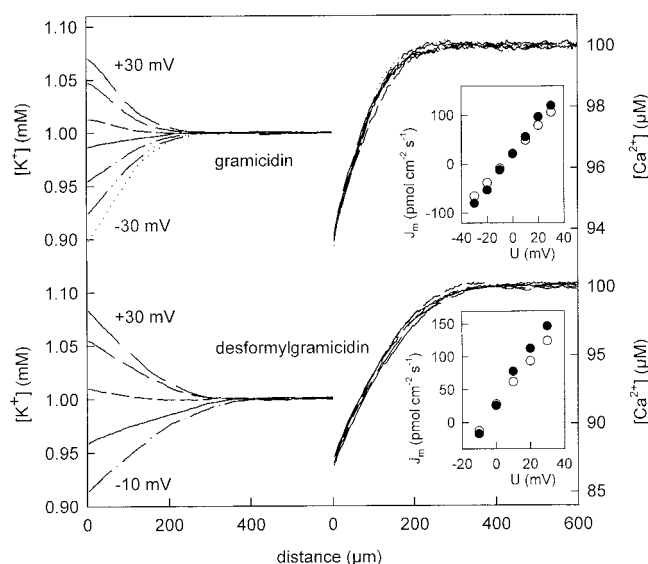


FIGURE 1 Representative calcium and potassium concentration distributions in the vicinity of planar membranes containing desformylgramicidin and gramicidin A channels. The profiles were recorded in the hypertonic compartment (0.8 M urea) under short-circuited conditions. The water flux across both the lipid bilayer and the peptide channels swept solute away from the membrane. The water flux,  $J_{W,c}$ , introduced by the porous pathway did not depend on the transmembrane potential applied. As calculated from the  $\text{Ca}^{2+}$  concentration profiles, gramicidin A accounted for  $0.1 \mu\text{mol cm}^{-2}\text{s}^{-1}$  and desformylgramicidin for  $1 \mu\text{mol cm}^{-2}\text{s}^{-1}$  of total water flux. The voltage-dependent potassium ion fluxes,  $J_m$ , across both types of channels were obtained from the transmembrane current density,  $I = J_m z F$ , measured ( $\circ$ ) and the concentration distribution of the permeable ion (Eq. 2,  $\bullet$ ). The buffer solutions contained 20 mM TRIS, 150 mM choline chloride, 1 mM KCl, and  $100 \mu\text{M Ca}^{2+}$ . pH was 8.4. Gramicidin A and desformyl-gramicidin concentrations were 12.5 and 740 ng/ml, respectively.

square residuals the program SigmaPlot was used.  $v_t$  consists of two terms, the velocity of water flow across the lipid,  $v_l$ , and across the channel,  $\Delta v$ ,

$$J_w = v_t/V_w = J_{w,l} + J_{w,c} = (v_l + \Delta v)/V_w, \quad (5)$$

where  $V_w$  is the partial molar volume of water. In the example shown in Fig. 1, gramicidin A accounts for  $0.1 \mu\text{mol cm}^{-2}\text{s}^{-1}$ , desformylgramicidin for  $1 \mu\text{mol cm}^{-2}\text{s}^{-1}$  of total water flux.  $J_w$  did not depend on the transmembrane potential applied. Because most of the channels are ion free at the low salt concentration chosen, this result was expected. Across both types of channels, a voltage-dependent potassium ion flux was observed (Fig. 1) as calculated according to Eq. 2 from  $v_t$  and the concentration distribution of the permeable ion. The transmembrane ion movement induced by a small potential of only 20 mV was sufficient not only to compensate for the solute dilution at the hypertonic side of the membrane but also to mediate an accumulation of the solute (Fig. 1). Obviously, the desformyl channel exhibits a larger water permeability than the gramicidin channel, whereas the ionic conductance seems to be

comparable. From the data shown in Fig. 1, an exact quantitative comparison of the hydraulic and ionic conductivities of gramicidin A and desformylgramicidin is not possible. Due to the large polarization effects that develop in a steady-state electric field, the membrane conductivity is underestimated. Therefore, the latter does not reflect the number of open channels that is usually obtained as the ratio of the membrane conductance and the single-channel conductance. To overcome this limitation, in the following experiments, membrane resistance is derived from short current pulses (Figs. 5–8). Additionally, the single-channel conductivity of the desformylgramicidin channel is monitored and compared with the one of gramicidin channel (Figs. 2–4).

### Proton permeability of desformylgramicidin

Voltage clamp ( $U = 100$  mV) measurements were undertaken in an acidic medium (pH 2.5) containing 100 mM choline chloride. At an aqueous concentration of 10 nM desformylgramicidin, the integral conductance of the lipid bilayer was approximately  $3 \cdot 10^{-6} \Omega^{-1}$ . Attaching a patch

pipette to the BLM enabled single-channel recordings (Fig. 2 A). The channel activity of desformylgramicidin under these conditions is characterized by current bursts flickering with a duration time of tens of seconds and records of silent patch (the end of the record in Fig. 2 A). The fraction of time open during the burst is rather high (about 0.8). As calculated from the histogram (Fig. 2 A), the probability of the channel being in the open state,  $\gamma$ , was equal to 0.5. It was found as the time open divided by the entire duration of the record (here 32 s). Single-channel conductance was 17.0 pS. Single-channel current depends linearly on the applied voltage (Fig. 2 B).

To compare the proton-conducting activities of desformylgramicidin and gramicidin A, current traces were recorded under identical conditions (Fig. 3). At an aqueous concentration of 2 nM, gramicidin A induced an integral membrane conductance of approximately  $0.1 \cdot 10^{-6} \Omega^{-1}$ . Again, a patch pipette was attached to the BLM to monitor the current across single channels (Fig. 3 A). Conductance and corresponding average duration time of the predominant transitions were 25 pS and 0.30 s, respectively.  $\gamma$  was equal to 0.1, i.e., the open-state probability of gramicidin A is smaller than the one of desformylgramicidin (see Figs.

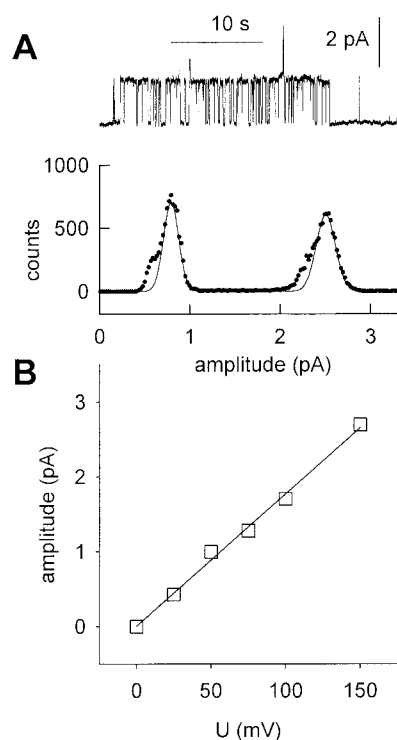


FIGURE 2 (A) Experimental record of proton current through desformylgramicidin channels. In the corresponding histogram (*squares*), the event number versus the conductance levels is shown. The Gaussian fit (*solid line*) returns mean peaks at 0.81 pA (baseline) and 2.50 pA (one open channel). The membrane patch was clamped at a voltage of 100 mV. (B) Voltage dependence of single-channel current. The solution contained 100 mM Choline chloride and 10 nM of the channel-former. pH of 2.5 was adjusted by addition of HCl.

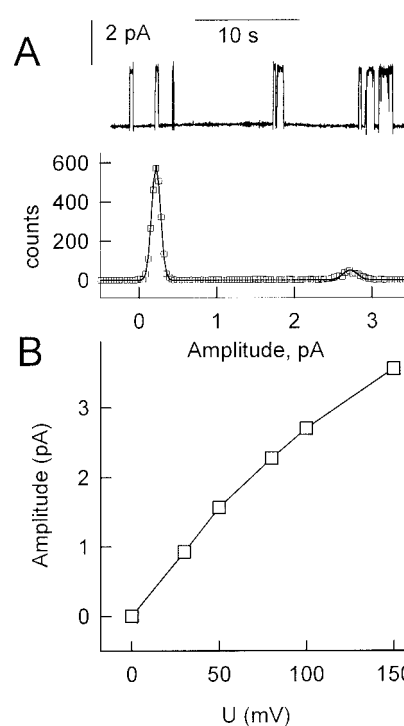


FIGURE 3 (A) Experimental record of proton current through gramicidin A channels. In the corresponding histogram (*squares*), the event number versus the conductance levels is shown. The Gaussian fit (*solid line*) returns mean peaks at 0.22 pA (baseline) and 2.71 pA (one open channel). The membrane patch was clamped at a voltage of 100 mV. (B) Voltage dependence of single-channel conductance. pH of the 100 mM choline chloride solution was 2.5. Gramicidin A was added in a concentration of 2 nM.

2 A and 3 A). At least in part, this difference is responsible for the higher integral conductivity,  $G$ , required to measure single desformylgramicidin channels.

### Cation permeability of desformylgramicidin

In contrast to single proton-conducting channels, single potassium or sodium channels were not observed with desformylgramicidin. This finding is in line with results reported earlier by Bezrukov (1984). The authors were unable to attribute the current fluctuations they have observed to any desformylgramicidin channel activity. With increasing peptide concentration, we now have detected an increasing patch conductance. A representative record of current through a patch is presented in Fig. 4 A. At a current level of about 14 pA (the transmembrane voltage was equal to 100 mV) two qualitatively different events can be distinguished: fast flickering that corresponds to repetitive openings and closings of a channel and long-lasting (measurable in minutes!) current steps; an example can be seen in the

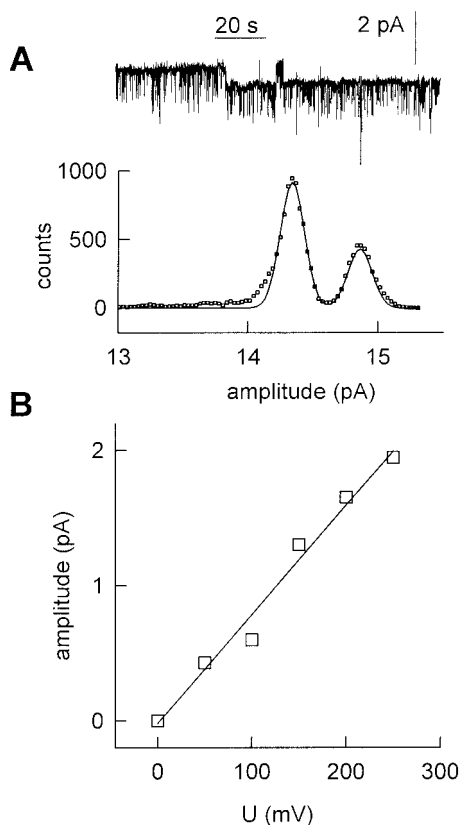


FIGURE 4 (A) Experimental record of potassium current through desformylgramicidin channels. In the corresponding histogram (*squares*), the event number versus the conductance levels is shown. The Gaussian fit (*solid line*) returns mean peaks at 14.30 pA (baseline) and 14.82 pA (one additional open channel). The multiple channel-containing membrane patch was clamped at a voltage of 100 mV. (B) Voltage dependence of single-channel conductance. The solution contained 100 mM KCl.

upper edge of Fig. 4 A. Similar to usual channel activity, the time-distribution histogram shows two peaks corresponding to a channel amplitude of 0.53 pA. The latter can be attributed to long-life single channels of desformylgramicidin.

From the ratio of patch and single-channel conductances, the number of open channels shown in the record (Fig. 4 A) is calculated to be  $\sim 26$ . About 30 s (average over 19 events) elapses between channel opening and subsequent channel closing. The conductance of the desformyl channels is a linear function of the applied voltage (Fig. 4 B), the average conductivity being 7 pS. Measurements in 100 mM NaCl solutions exhibited qualitatively similar results. A single-channel conductance of 3 pS was obtained (data not shown).

### Single-channel hydraulic permeability coefficient

Channel insertion into a short-circuited membrane was accompanied by an increase of the osmotically induced near-membrane polarization of both the permeable and impermeable cations (Fig. 5). The flux of the monovalent ion across the desformylgramicidin channel was too small to compensate for the dilution occurring due the water flux. With gramicidin A, the opposite phenomenon had been observed. Due to the overwhelming increase in cation conductance, the concentration gradients of the monovalent cations dissipated at a very large channel density (Pohl and Saparov, 2000). This observation allows one to conclude that desformylgramicidin facilitates water movement more efficiently than does gramicidin A. The hydraulic membrane conductivity of the membrane,  $P_F$ , is represented as the sum of the water permeabilities of the lipid bilayer,  $P_{f,l}$ ,

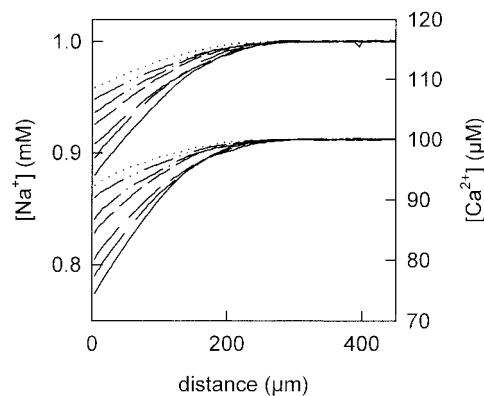


FIGURE 5 Osmosis-mediated dilution of two different solutes in the membrane vicinity under short-circuited conditions. The dotted line denotes profiles near the unmodified bilayer. After insertion of desformylgramicidin, the polarization of both  $\text{Ca}^{2+}$  and  $\text{Na}^+$  increases. The augmentation of the desformylgramicidin concentration is indicated by the length of the dashes reaching a maximum ( $1.4 \mu\text{g/ml}$ ) with the spline line. The buffer solutions contained 20 mM TRIS, 150 mM choline chloride, 1 mM NaCl, and  $100 \mu\text{M Ca}^{2+}$ . pH was 8.4. 0.8 M urea was added to the *trans*-compartment.

and of the channel,  $P_{f,c}$ :

$$P_f = P_{f,l} + P_{f,c} = \frac{v_1}{\chi c_{\text{osm}} V_w} + \frac{\Delta v}{\chi c_{\text{osm}} V_w}, \quad (6)$$

where  $\chi$  and  $c_{\text{osm}}$  are the osmotic coefficient (0.93 for urea) and the near-membrane concentration of the solute used to establish the transmembrane osmotic pressure difference, respectively. Plotting  $P_{f,c}$  as a function of the corresponding electrical membrane conductivity,  $G$ , allows finding of the single-channel hydraulic permeability coefficient,  $p_f$ , for the desformylgramicidin pore (Fig. 6):

$$p_f = \frac{P_f A}{n} = \frac{P_{f,c} A g}{G}, \quad (7)$$

where  $A$  is the membrane area (Finkelstein, 1987). From the slopes of the linear regressions in 1 mM NaCl or KCl,  $p_f$  was found to be equal to 1.0 and  $1.3 \cdot 10^{-12} \text{ cm}^3 \text{ s}^{-1}$ , respectively. For the calculations according to Eq. 6, the measured single-channel conductance was corrected for the lower electrolyte concentration used in our experiments according to Neher et al. (1978). For 1 mM NaCl and KCl, a single-channel conductance of 0.07 and 0.13 pS, respectively, was assumed. Because  $c_{\text{osm}}$  cannot be measured directly, it was derived from  $c_{i,s}$ ,  $c_{i,b}$ ,  $D_{\text{osm}}$ , and  $D_i$ , the near-membrane and bulk concentrations of the impermeable cation, the diffusion coefficients of the osmolyte and the impermeable cation, respectively (Pohl and Saparov, 2000):

$$\sqrt[3]{\frac{D_i^2}{D_{\text{osm}}^2} \left[ 1 - \frac{c_{i,b}}{c_{i,s}} \right]} = 1 - \frac{c_{\text{osm},b}}{c_{\text{osm}}}. \quad (8)$$

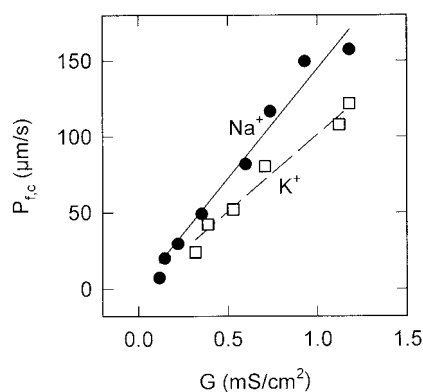


FIGURE 6 Determination of the single-pore water permeability coefficient. From calcium concentration profiles obtained during three runs of the experiment shown in Fig. 5 and two analogous experiments in which sodium (●) was substituted for potassium (□), the desformylgramicidin-mediated increase in the hydraulic membrane conductance  $P_{f,c}$  was calculated. Based on the membrane conductance  $G$  measured and the single-channel conductance determined earlier (Fig. 4), the single-pore water permeability coefficient was derived to be  $1 \cdot 10^{-12} \text{ cm}^3 \text{ s}^{-1}$  (●) or  $1.3 \cdot 10^{-12} \text{ cm}^3 \text{ s}^{-1}$  (□).

## Competition of ion and water flow

A difference between  $\text{K}^+$  or  $\text{Na}^+$  bulk concentrations at the hypertonic and the hypotonic sides of the membrane was established to compensate for both solute accumulation on one side of the membrane and depletion (record I in Figs. 7 and 8) on the other side, which accompany water movement across the membrane. The bulk concentration in the hyperosmotic compartment was adjusted to get equal cation concentrations at both membrane/water interfaces (record II in Figs. 7 and 8). This procedure was repeated for different osmolyte concentrations (record III in Fig. 7 and records III and IV in Fig. 8). The transmembrane ion flux measured in the absence of concentration gradient across the membrane,  $J_{m,t}$  is due solely to solvent drag. The number of water molecules that are required to drag one ion across the channel can be derived from their transmembrane ion flux measured along with membrane conductivity (Pohl and Saparov, 2000):

$$J_{m,t} = RT\chi c_{\text{osm}} V_w N G / z^2 F^2. \quad (9)$$

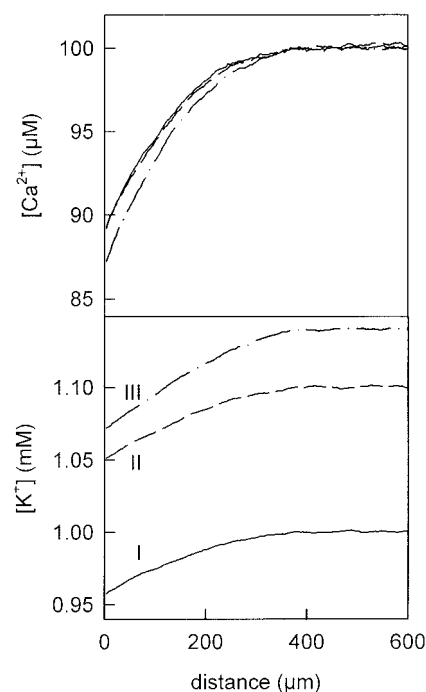


FIGURE 7 Number of water molecules  $N$  that are transported in single-file fashion along with one potassium ion across the desformylgramicidin channel. Under short-circuited conditions (experiment I) potassium (1 mM in the *cis* and *trans* bulk solutions) is dragged by the osmotic water flow across desformylgramicidin channels and flows along its concentration gradient (*spline line*). The latter is zero after the bulk concentration of KCl at the hypertonic side had been augmented to 1.1 mM (experiment II). After an increase of the urea concentration from 0.8 to 1 M in the hypertonic compartment, a true solvent drag situation was found again at a potassium concentration of 1.4 mM (experiment III). With respect to the simultaneously measured membrane conductivity of  $0.2 \text{ mS cm}^{-2}$ , the number of water molecules moving along with one cation is calculated to be 4.5 from experiments II and III.

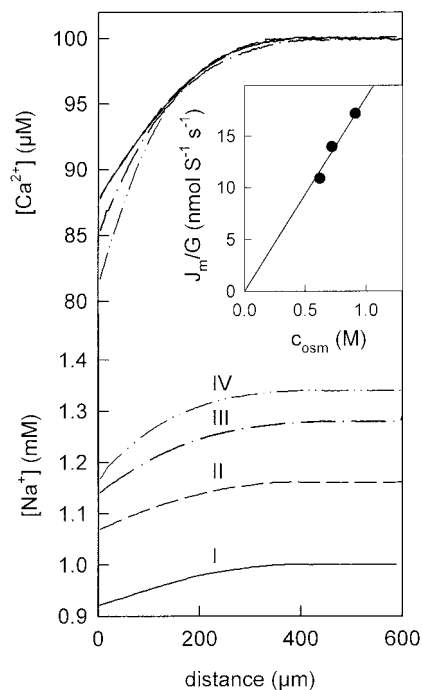


FIGURE 8 Number of water molecules  $N$  transported along with one sodium ion. The experiment from Fig. 7 was repeated substituting  $\text{Na}^+$  for  $\text{K}^+$ . Pseudo solvent drag that was observed under these conditions (experiment I) disappeared after augmenting the *trans* NaCl concentration to 1.16, 1.28, and 1.34 mM at 0.8 (experiment II), 1 (experiment III), and 1.2 (experiment IV) M urea. The amount of sodium ions  $J_m$  that is dragged through the membrane with conductance  $G$  is proportional to the effective osmotic gradient  $c_{\text{osm}}$  (see inset). From the slope,  $N$  was calculated to be 4.8.

From the potassium (Fig. 7) and sodium (Fig. 8) fluxes measured under these conditions, respectively,  $4.5 \pm 0.3$  and  $4.8 \pm 0.3$  (4 independent experiments for each ion), water molecules were found to be transported simultaneously with one ion through the channel.

## DISCUSSION

Desformylgramicidin was found to exhibit a higher water selectivity than did gramicidin A, i.e., their ratios of water to ion conductivities differ by about two orders of magnitude. The difference does not result from deviations in the single-channel ion conductance but rather from the large single-channel water permeability coefficient of desformylgramicidin. The transport rate of  $1.1 \cdot 10^{-12} \text{ cm}^3 \text{ s}^{-1}$  is five times greater than the maximum single-channel water permeability predicted from Eq. 1. The peptide shares the unusual high water permeability with human AQP4 and *E. coli* AQPZ water channel proteins (Yang and Verkman, 1997; Borgnia et al., 1999). Also, for AQP4, the simplistic equations derived for idealized cylindrical, noninteractive water pores were therefore found to be probably inadequate to provide useful information about the molecular mechanism

of water permeation (Yang et al., 1997). However, the finding that desformylgramicidin also does not fit into the current pore model of single-file transport (Eq. 1) questions the explanation given for the high hydraulic conductivity of AQP4, i.e., the hypothesized need for protein assembly in orthogonal arrays (Yang et al., 1997).

Differences in pore structure between gramicidin and desformylgramicidin channels may be supposed to account for the higher water permeability of the latter. However, gramicidin A is assumed to impose negligible resistance to water movement within the pore. In molecular dynamics simulations, the overall water permeation rate was found to be much lower than it would be if there were no significant resistance beyond that of the channel lumen itself (Chiu et al., 1999). Assuming that the divergence between the water permeabilities through gramicidin channels imbedded into phospholipids (Rosenberg and Finkelstein, 1978b) and glycerols (Dani and Levitt, 1981b) is due to the net different hydration environment for water just outside the channel mouth in the two environments (Chiu et al., 1999), a positive charge at the channel mouth could be hypothesized to contribute to the large hydraulic conductivity of the peptide. Only if the desformyl channel adopts a double-stranded conformation (Fig. 9), the positive charge of the N-terminus would be located at the channel entrance and could alter the rate at which water can transform its hydration environment



FIGURE 9 Desformyl derivatization of gramicidin A. The removal of the formyl group ( $-\text{HC}=\text{O}$ ) gives a plus charge at the N-terminal of the peptide. It is represented by the  $-\text{NH}_3^+$  shown in the figure. Theoretically, two different folding motives can form the active channel: (A) two single-stranded helices or (B) a double-stranded helix. Indirect evidence was obtained that favors the configuration shown in B.

from that of the channel interior to that of the exterior, thereby lowering the access resistance for water.

The double-stranded dimer was suggested to form the active channel based on mitochondria uncoupling mediated by desformylgramicidin (Rottenberg and Koeppel, 1989). This is plausible because it is energetically unfavorable to bury the positive N-termini into the hydrophobic membrane environment and to bring them close together in the membrane-spanning channel, i.e. in the case of desformylgramicidin, a head-to-head dimer of two single-stranded helices is unlikely. In the absence of independent structural data, this hypothesis cannot be considered proven. However, in the present work, several indirect arguments in favor of such a folding motif are obtained:

1. The failure of the desformylgramicidin peptide to exclude protons and cations from penetrating the channel suggests that the positive charge of the N-terminus is not located within the narrow pore.
2. The desformylgramicidin derivative exhibits a long channel lifetime (Figs. 2 and 4) that is similar to chiral mismatched gramicidins. The latter are known to form also double-stranded heterodimers (Durkin et al., 1992).
3. Finally, fast flickering of single-channel conductance also is observed for double-stranded channels of gramicidin A itself in very thick membranes (Mobashery et al., 1997).

Summarizing, with respect to its very high single-channel hydraulic permeability, desformylgramicidin may serve as a model for extremely permeable natural water-channel proteins (AQP4 and AQPZ). The mechanism responsible for the low access resistance to water remains to be analyzed with closely related gramicidin analogues.

Financial support of the Deutsche Forschungsgemeinschaft (Po 533/2-2; 436RUS113/60) is gratefully acknowledged.

## REFERENCES

- Akeson, M. and D. W. Deamer. 1991. Proton conductance by the gramicidin water wire: model for proton conductance in the F-1F<sub>0</sub> ATPases? *Biophys. J.* 60:101-109.
- Amman, D. 1986. Ion-Selective Microelectrodes. Principles, Design and Application. Springer, Berlin.
- Andersen, O. S., H. J. Apell, E. Bamberg, D. D. Busath, R. E. Koeppel, F. J. Sigworth, G. Szabo, D. W. Urry, and A. Woolley. 1999a. Gramicidin channel controversy—the structure in a lipid environment. *Nat. Struct. Biol.* 6:609-609.
- Andersen, O. S., D. V. Greathouse, L. L. Providence, M. D. Becker, and R. E. Koeppel. 1998. Importance of tryptophan dipoles for protein function: 5-fluorination of tryptophans in gramicidin A channels. *J. Am. Chem. Soc.* 120:5142-5146.
- Andersen, O. S., C. Nielsen, A. M. Maer, J. A. Lundbaek, M. Goulian, and R. E. Koeppel. 1999b. Ion channels as tools to monitor lipid bilayer-membrane protein interactions: gramicidin channels as molecular force transducers. *Methods Enzymol.* 294:208-224.
- Antonenko, Y. N., and A. A. Bulychev. 1991. Measurements of local pH changes near bilayer lipid membrane by means of a pH microelectrode and a protonophore-dependent membrane potential—comparison of the methods. *Biochim. Biophys. Acta.* 1070:279-282.
- Antonenko, Y. N., G. A. Denisov, and P. Pohl. 1993. Weak acid transport across bilayer lipid membrane in the presence of buffers—theoretical and experimental pH profiles in the unstirred layers. *Biophys. J.* 64:1701-1710.
- Antonenko, Y. N., and P. Pohl. 1998. Coupling of proton source and sink via H<sup>+</sup>-migration along the membrane surface as revealed by double patch-clamp experiments. *FEBS Lett.* 429:197-200.
- Bezrukov, S. M., A. I. Irkhin, and E. Melnik. 1984. Desformylgramicidin a proton selective channel. *Biol. Membrany.* 1:659-665.
- Borgnia, M. J., D. Kozono, G. Calamita, P. C. Maloney, and P. Agre. 1999. Functional reconstitution and characterization of AQPZ, the *E. coli* water channel protein. *J. Mol. Biol.* 291:1169-1179.
- Busath, D. D., C. D. Thulin, R. W. Hendershot, L. R. Phillips, P. Maughan, C. D. Cole, N. C. Bingham, S. Morrison, L. C. Baird, R. J. Hendershot, M. Cotten, and T. A. Cross. 1998. Noncontact dipole effects on channel permeation. I. Experiments with (5F-Indole)Trp(13) gramicidin A channels. *Biophys. J.* 75:2830-2844.
- Chiu, S. W., S. Subramaniam, and E. Jakobsson. 1999. Simulation study of a gramicidin/lipid bilayer system in excess water and lipid. II. Rates and mechanisms of water transport. *Biophys. J.* 76:1939-1950.
- Dani, J. A., and D. G. Levitt. 1981a. Water transport and ion-water interaction in the gramicidin channel. *Biophys. J.* 35:501-508.
- Dani, J. A., and D. G. Levitt. 1981b. Binding constants of Li<sup>+</sup>, K<sup>+</sup>, and Tl<sup>+</sup> in the gramicidin channel determined from water permeability measurements. *Biophys. J.* 35:485-499.
- Durkin, J. T., L. L. Providence, R. E. Koeppel, and O. S. Andersen. 1992. Formation of non-β<sup>6,3</sup>-helical gramicidin channels between sequence-substituted gramicidin analogues. *Biophys. J.* 62:145-157.
- Fettiplace, R. and D. A. Haydon. 1980. Water permeability of lipid membranes. *Physiol. Rev.* 60:510-550.
- Finkelstein, A. 1987. Water Movement through Lipid Bilayers, Pores, and Plasma Membranes. Wiley and Sons, New York. 42-749.
- Finkelstein, A., and O. S. Andersen. 1981. The gramicidin A channel: a review of its permeability characteristics with special reference to the single-file aspect of transport. *J. Membrane Biol.* 59:155-171.
- Goodall, M. C. 1971. Thickness dependence in the action of gramicidin A on lipid bilayers. *Arch. Biochem. Biophys.* 147:129-135.
- Goulian, M., O. N. Mesquita, D. K. Fygenson, C. Nielsen, O. S. Andersen, and A. Libchaber. 1998. Gramicidin channel kinetics under tension. *Biophys. J.* 74:328-337.
- Greathouse, D. V., R. E. Koeppel, L. L. Providence, S. Shobana, and O. S. Andersen. 1999. Design and characterization of gramicidin channels. *Methods Enzymol.* 294:525-550.
- Hladky, S. B., and D. A. Haydon. 1984. Ion movements in gramicidin channels. *Curr. Top. Membr. Transp.* 21:327-372.
- Ismailov, I. I., V. G. Shlyonsky, and D. J. Benos. 1997. Streaming potential measurements in αβγ-rat epithelial Na<sup>+</sup>-channel in planar lipid bilayers. *Proc. Natl. Acad. Sci. U. S. A.* 94:7651-7654.
- Ketchem, R. R., B. Roux, and T. A. Cross. 1997. High resolution polypeptide structure in a lamellar phase lipid environment from solid state NMR derived orientational constraints. *Structure.* 5:1655-1669.
- Koeppel, R. E., and O. S. Andersen. 1996. Engineering the gramicidin channel. *Annu. Rev. Biophys. Biomol. Struct.* 25:231-258.
- Koeppel, R. E., J. A. Paczkowski, and W. L. Whaley. 1985. Gramicidin K, a new linear channel-forming gramicidin from *Bacillus brevis*. *Biochemistry.* 24:2822-2826.
- Levitt, D. G., S. R. Elias, and J. M. Hautman. 1978. Number of water molecules coupled to the transport of sodium, potassium and hydrogen ions via gramicidin, nonactin or valinomycin. *Biochim. Biophys. Acta.* 512:436-451.
- Marsh, D. 1996. Peptide models for membrane channels. *Biochem. J.* 315:345-361.
- Mathai, J. C., S. Mori, B. L. Smith, G. M. Preston, N. Mohandas, M. Collins, P. C. van-Zijl, M. L. Zeidel, and P. Agre. 1996. Functional analysis of aquaporin-1 deficient red cells. The Colton-null phenotype. *J. Biol. Chem.* 271:1309-1313.

- Miller, C. 1982. Coupling of water and ion fluxes in a  $K^+$ -selective channel of sarcoplasmic reticulum. *Biophys. J.* 38:227–230.
- Mobashery, N., C. Nielsen, and O. S. Andersen. 1997. The conformational preference of gramicidin channels in a function of lipid bilayer thickness. *FEBS Lett.* 412:15–20.
- Mueller, P., D. O. Rudin, H. T. Tien, and W. C. Wescott. 1963. Methods for the formation of single bimolecular lipid membranes in aqueous solution. *J. Phys. Chem.* 67:534–535.
- Neher, E., J. Sandblom, and G. Eisenman. 1978. Ionic selectivity, saturation, and block in gramicidin A channels. II. Saturation behavior of single-channel conductances and evidence for the existence of multiple binding sites in the channel. *J. Membrane Biol.* 40:97–116.
- Pohl, P., Y. N. Antonenko, and E. H. Rosenfeld. 1993. Effect of ultrasound on the pH profiles in the unstirred layers near planar bilayer lipid membranes measured by microelectrodes. *Biochim. Biophys. Acta.* 1152:155–160.
- Pohl, P., and S. M. Saparov. 2000. Solvent drag across gramicidin channels demonstrated by microelectrodes. *Biophys. J.* 78:2426–2434.
- Pohl, P., S. M. Saparov, and Y. N. Antonenko. 1997. The effect of a transmembrane osmotic flux on the ion concentration distribution in the immediate membrane vicinity measured by microelectrodes. *Biophys. J.* 72:1711–1718.
- Preston, G. M., T. P. Carroll, W. B. Guggino, and P. Agre. 1992. Appearance of water channels in *Xenopus* oocytes expressing red cell CHIP28 protein. *Science.* 256:385–387.
- Rosenberg, P. A., and A. Finkelstein. 1978a. Interactions of ions and water in gramicidin A channels. Streaming potentials across lipid bilayer membrane. *J. Gen. Physiol.* 72:327–340.
- Rosenberg, P. A., and A. Finkelstein. 1978b. Water permeability of gramicidin A-treated lipid bilayer membranes. *J. Gen. Physiol.* 72:341–350.
- Rottenberg, H., and R. E. Koeppe. 1989. Stimulation of cation transport in mitochondria by gramicidin and truncated derivatives. *Biochemistry.* 28:4361–4367.
- Tripathi, S., and S. B. Hladky. 1998. Streaming potentials in gramicidin channels measured with ion-selective microelectrodes. *Biophys. J.* 74:2912–2917.
- Tu, Q., P. Velez, M. Brodwick, and M. Fill. 1994. Streaming potentials reveal a short ryanodine-sensitive selectivity filter in cardiac  $Ca^{2+}$  release channel. *Biophys. J.* 67:2280–2285.
- Walz, T., B. L. Smith, M. L. Zeidel, A. Engel, and P. Agre. 1994. Biologically active two-dimensional crystals of aquaporin chip. *J. Biol. Chem.* 269:1583–1586.
- Weiss, L. B., and R. E. Koeppe. 1985. Semisynthesis of linear gramicidins using diphenyl phosphorazidate (DPPA). *Int. J. Pept. Protein. Res.* 26:305–310.
- Yang, B., and A. S. Verkman. 1997. Water and glycerol permeabilities of aquaporins 1–5 and MIP determined quantitatively by expression of epitope-tagged constructs in *Xenopus* oocytes. *J. Biol. Chem.* 272:16140–16146.
- Yang, B. X., A. N. Vanhoek, and A. S. Verkman. 1997. Very high single channel water permeability of aquaporin-4 in baculovirus-infected insect cells and liposomes reconstituted with purified aquaporin-4. *Biochemistry.* 36:7625–7632.
- Zeidel, M. L., S. Nielsen, B. L. Smith, S. V. Ambudkar, A. B. Maunsbach, and P. Agre. 1994. Ultrastructure, pharmacologic inhibition, and transport selectivity of aquaporin channel-forming integral protein in proteoliposomes. *Biochemistry.* 33:1606–1615.